08

Adsorption of organic macromolecule on free-standing and epitaxial graphene having gap in electronic spectrom

© S.Yu. Davydov,[1] O.V. Posrednik[2]

[1]Ioffe Institute,
194021 St. Petersburg, Russia
[2]St. Petersburg State Electrotechnical University „LETI“,
197022 St. Petersburg, Russia
e-mail: Sergei_Davydov@mail.ru

Received October 14, 2024
Revised October 14, 2024
Accepted October 14, 2024

The contact of an organic macromolecule (MM) with free-standing and epitaxial graphene hav-ing gap in the electronic spectrum is considered within the framework of the previously proposed dangling bond model (S.Yu. Davydov. Phys. Solid State, 64, 2018 (2022)) and the HOMO-LUMO model. The main attention is paid to local states in the gap that arise due to the adsorption of MM, for whose energy and occupation numbers analytical expressions are obtained. SiC polytypes are considered as graphene substrates. The possibility of using gapped graphene in resistive biosensors is briefly discussed.

Keywords: macromolecule, gapped graphene, SiC polytypes, local states.

DOI: 10.61011/TP.2025.03.60857.324-24

Introduction

In the context of a recent increase in interest in biosensors, a model of adsorption (adhesion) of an organic macromolecule (MM) on ideal (gapless) single-layer graphene (SLG) was proposed in [1]. It was assumed in the dangling bond model (DBM) proposed in [1] that the interaction of MMs with SLG is mediated by dangling molecular bonds of MM fragments adjacent to SLG (or cross-links). DBM provided an opportunity to estimate the charge transfer between MMs and SLG, which, in turn, made it possible to estimate the energy of adsorption (adhesion) of MMs on SLG. In the present study, we examine MM-SLG coupling and how a gap in the SLG electronic spectrum affects the charge transfer between MMs and the graphene substrate.

Let us consider the adsorption of MMs on free-standing gapped graphene within DBM. A gap in free-standing SLG may be opened by applying an external mechanical stress to a graphene sheet [2]. After this, we move on to epitaxial graphene with a gap in its spectrum induced by a semiconductor substrate [3] and consider the adsorption of MMs within the HOMO-LUMO (higher occupied and lower unoccupied molecular orbital) model [4].

The semiconductor substrate-SLG-MM structure obtained this way represents a model of a biosensor in its initial state (when the tested biomolecule has not yet been brought into contact with an MM) [5]. The detection signal of a resistive sensor is the change in current flowing along SLG induced by the tested biomolecule. The analytical theory of operation of a biosensor based on gapless graphene [5] is used to discuss briefly the effects introduced by a gap, although it is a priori clear that the conductivity of gapless graphene is metallic in nature, while gapped graphene has an activation (semiconductor) conductivity.

1. Macromolecule on free-standing gapped graphene in the DBM model

Let us consider an MM adsorbed on free-standing gapped graphene first. We present the Hamiltonian of such a system in the form

$$H = \sum_{\mathbf{k}} \varepsilon_{gap}(\mathbf{k}) c_{\mathbf{k}}^{+} c_{\mathbf{k}} \sum_{i} \varepsilon_i a_i^{+} a_i + \sum_{i,\mathbf{k}} \frac{V_i^2 (c_{\mathbf{k}}^{+} a_i + a_i^{+} c_{\mathbf{k}})}{\omega - \varepsilon_{SLG}(\mathbf{k}) + i0^{+}}, \quad (1)$$

where dispersion law $\varepsilon_{gap}(\mathbf{k})$ in the low-energy approximation is written as

$$\varepsilon_{gap}(\mathbf{k}) = \pm\sqrt{\Delta^2 + (3tka/2)^2}, \quad (2)$$

2Δ — gap width, $\mathbf{k}$ — wave vector measured from the wave vector of the Dirac point to which energy $\varepsilon_D = 0$ is ascribed, and t — energy of electron hopping between nearest neighbors in graphene separated by distance $a = 1.42$ Å. ε_i — energy of the ith dangling bond of the MM [1], V_i — energy of interaction of the ith bond with graphene, $c_{\mathbf{k}}^{+}(c_{\mathbf{k}})$ — operator of creation (annihilation) of an SLG electron in state $|\mathbf{k}\rangle$, and $a_i^{+}(a_i)$ — similar operators for the ith dangling bond. At $ka \ll 2\Delta/3t \sim 0.1$ (see below), spectrum (2) assumes a parabolic form $\varepsilon_{gap}(\mathbf{k}) \approx \pm\Delta \pm h^2k^2/2m^*$, where effective mass $m^* = 4\hbar^2\Delta/(3ta)^2$ and $\hbar$ is the reduced Planck constant. Figure 1 illustrates this scenario.

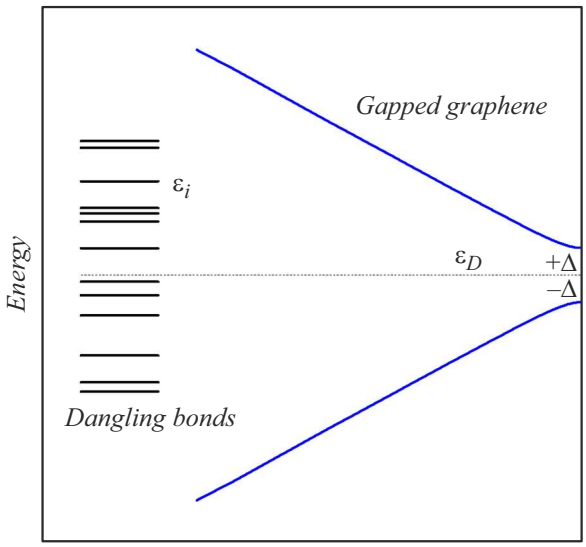

Figure 1. Energy diagram of MM adsorption on gapped graphene (ε_i — energy of the ith dangling bond of the MM, ε_D — Dirac point energy, and 2Δ — gap width; $\varepsilon_{gap}(\mathrm{k})$ dispersion is presented for $\mathrm{k} \leq 0$).

Owing to adsorption, the density of states (DOS) of an electron at the ith bond (per one spin projection) is

$$\rho_i^{gap}(\omega) = \frac{1}{\pi} \frac{\Gamma_i^{gap}(\omega)}{(\omega - \varepsilon_i - \Lambda_i^{gap}(\omega))^2 + (\Gamma_i^{gap}(\omega))^2}. \quad (3)$$

Here, ω is the energy variable, the broadening function of the ith quasi-level is $\Gamma_i^{gap}(\omega) = \pi V_i^2 \rho_{gap}(\omega)$, and the corresponding shift function $\Lambda_i^{gap}(\omega)$ is the Hilbert transform of function $\Gamma_i^{gap}(\omega)$, where DOS of gapped graphene $\rho_{gap}(\omega)$, according to Appendix 2 from [1], takes the form

$$\rho_{gap}(\omega) = \begin{cases} \dfrac{2|\omega|}{\xi^2}, & \sqrt{\xi^2 + \Delta^2} \geq |\omega| \geq \Delta, \\ 0, & |\omega| < \Delta, \quad |\omega| > \sqrt{\xi^2 + \Delta^2}, \end{cases} \quad (4)$$

so that the shift function is

$$\Lambda_i^{gap}(\omega) = \frac{2V_i^2}{\xi^2} \omega \ln \left| \frac{\omega^2 - \Delta^2}{\omega^2 - \Delta^2 - \xi^2} \right| \quad (5)$$

and $\xi = \sqrt{2\pi\sqrt{3}t}$ is the cutoff energy. At $\Delta = 0$, expressions (4) and (5) are transformed into formulae (4) and (5) from [1], where $\xi^2 = \xi^2/2$. The occupation number of the ith initially dangling bond at zero temperature is the sum

$$n_i^{gap} = (n_i^{gap})_{band} + (n_i^{gap})_{loc} \quad (6)$$

of the contribution of valence band i of graphene

$$(n_i^{gap})_{band} = 2 \int\limits_{-\sqrt{\xi^2+\Delta^2}}^{-\Delta} \rho_i^{gap}(\omega) d\omega \quad (7)$$

and the contribution of a local level located in the gap with its energy written as

$$\varepsilon_i^{loc} = \varepsilon_i + \Lambda_i^{gap}(\varepsilon_i^{loc}), \quad (8)$$

which is given by

$$(n_i^{gap})_{loc} = \nu_i^{loc} \Theta(\mu - \varepsilon_i^{loc}),$$
$$\nu_i^{loc} = 2 \left| 1 - \frac{d\Lambda_i^{gap}(\omega)}{d\omega} \right|_{\varepsilon_i'}^{-1}, \quad (9)$$

where $\Theta(\ldots)$ is the Heaviside function, ν_i^{loc} is the fill factor, and μ is the chemical potential. It is easy to demonstrate that

$$\frac{d\Lambda_i^{gap}(\omega)}{d\omega} = \frac{2V_i^2}{\xi^2} \left[\ln \left| \frac{\omega^2 - \Delta^2}{\omega^2 - \Delta^2 - \xi^2} \right| + \frac{2\omega^2\xi^2}{(\omega^2 - \Delta^2)(\omega^2 - \Delta^2 - \xi^2)} \right]. \quad (10)$$

Note that the adsorption on binary graphene-like compounds (GLCs) of the $A_N B_{8-N}$ type was discussed in detail in [17]. Since GLCs differ from gapped graphene only in the nature of the gap (its half-width being equal to $\Delta_{AB} = |\varepsilon_A - \varepsilon_B|/2$, where $\varepsilon_{A(B)}$ is the energy of the p orbital of atom $A(B)$), it follows from a comparison of the results [12,17] that the main difference between gapped and gapless graphene consists in the presence of local states the energy of which is determined from Eq. (8). Its graphical solution was presented in Fig. 1, *b* in [17]. A detailed analysis of the occupation numbers under varying problem parameters was also performed in [17] (see Figs. 2–4). In the present study, we limit ourselves to order-of-magnitude estimates.

Since $t \sim 3\,\mathrm{eV}$ and $\xi \sim 10\,\mathrm{eV}$, it follows from Table 2 presented in review [3] that relation $\Delta^2/\xi^2 \ll 1$ holds true in graphene in the overwhelming majority of cases. It is then easy to demonstrate that the band contributions to the dangling bond occupation numbers for gapped and gapless graphene match to within $\sim \Delta^2/\xi^2$. At $\Delta^2/\xi^2 \ll 1$ and $\omega^2 < \Delta^2$, shift function (5) is substituted with $\Lambda_i^{gap} \approx -(2V_i^2\omega/\xi^2)\ln[\xi^2/(\Delta^2 - \omega^2)]$. As for local states, $d\Lambda_i^{gap}/d\omega \approx -(2V_i^2/\xi^2)\left[\ln[\xi^2/(\Delta^2 - \omega^2)] + 2\omega^2/(\Delta^2 - 1\omega^2)\right]$ under the same conditions. Figure 2 shows typical dependences $\varepsilon_i^{loc}(\varepsilon_i)$ and $\nu_i^{loc}(\varepsilon_i)$. It is easy to demonstrate that $\varepsilon_i^{loc} \to -(2V_i^2\varepsilon/\xi^2)\ln(\xi^2/\Delta^2)$ and $\nu_i^{loc} \to (\nu_i^{loc})_{\max} = 2[1 + (2V_i^2/\xi^2)\ln(\xi^2/\Delta^2)]^{-1}$ at $\varepsilon_i \to \varepsilon_D$, while $\varepsilon_i^{loc} \to \mp\Delta$ and $\nu_i^{loc} \to 0$ are obtained at $\varepsilon_i \to \pm\infty$. Thus, it is the filling of local levels ε_i^{loc} that sets the difference in charge transfer between the MM-gapped graphene and MM-gapless graphene systems (see [17] for more details).

2. MM on epitaxial graphene. HOMO-LUMO model

Let us now turn to MMs adsorbed on epitaxial gapped graphene (gapped epigraphene). The exact expression

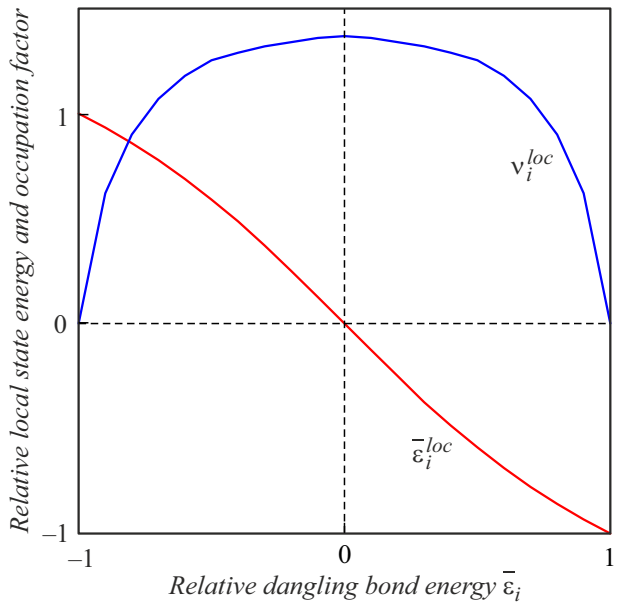

Figure 2. Free-standing graphene: dependences of reduced energy $\bar{\varepsilon}_i^{loc} = \varepsilon_i^{loc}/\Delta$ of the ith local state and factor ν_i^{loc} on reduced energy $\bar{\varepsilon}_i = \varepsilon_i/\Delta$ of the ith dangling bond.

for the DOS for epitaxial GLCs on semiconductors was obtained in [7]. It remains valid for gapped graphene, but is too cumbersome and inconvenient for further analysis. Therefore, we will make a number of simplifying assumptions.

Semiconductor substrate DOS $\rho_{sub}(\omega)$ is assumed to be characterized by the Haldane–Anderson model [8]:

$$\rho_{sub}(\Omega) = \begin{cases} \rho_{sc}, & |\Omega| \geq E_g/2, \\ 0, & |\Omega| < E_g/2, \end{cases} \qquad (11)$$

where $\rho_{sc} = \text{const}$, $\Omega = \omega - \omega_0$, and ω_0 is the center energy of a band gap with width E_g (Table 1). Thus, we obtain broadening functions $\Gamma_{sub}(\omega) = \pi V^2 \rho_{sc}$ at $|\Omega| \geq E_g/2$ and $\Gamma_{sub}(\omega) = 0$ at $|\Omega| \leq E_g/2$ and shift function $\Lambda_{sub}(\Omega) = \rho_{sc} V^2 \ln|(\Omega - E_g/2)/(\Omega + E_g/2)|$, where V is the matrix element of graphene–substrate coupling, for the electronic states of gapped graphene. The gapped graphene–semiconductor substrate system is a system of heterojunctions the energy diagrams of which are shown in Fig. 4.27 in [9]. According to [10–13], the width of the gap induced by a substrate is several tenths of an electronvolt for graphene on the surface of 4*H* and 6*H* SiC polytypes. The largest gap ($\sim 1.5\,\text{eV}$) forms when SLG is brought into contact with hexagonal two-dimensional boron nitride h-BN. Thus, it may be assumed that $\Delta^2/\xi^2 \ll 1$ also holds true for epigraphene. The values of ω_0 and the energy of the shifted (due to interaction with the substrate) Dirac point $\varepsilon'_D = -\Lambda_{sub}(0)$ obtained in [14] are listed in Table 1.

It follows from this table that energy interval $(-\Delta + \varepsilon'_D, \varepsilon'_D + \Delta)$ is located in the band gap of silicon carbide polytypes at $\Delta < \varepsilon'_D$. Thus, a type I straddling heterojunction is established (see [7] and Fig. 1, *b* in [9]). If the gap overlaps with the bands of allowed states, a type III broken heterojunction forms (see [7] and Fig. 1, *c* in [9]). This scenario is similar to the case of adsorption on a metal where the gap vanishes [15].

Let us simplify the analysis further and apply the formulae for free-standing gapped graphene from Section 1 with renormalization of the Dirac point $\varepsilon_D = 0 \to \varepsilon'_D$ (see Table 1) in the case of overlapping of the gap with the band of forbidden states (type I heterojunction). Thus, $\omega' = \omega - \varepsilon'_D$ should be used instead of energy ω in all the formulae of Section 1 [14]. It must be emphasized that the use of formula (3), which corresponds to free-standing graphene (and not GLC DOS [9]), for the DOS of epigraphene is valid only in the weak graphene–substrate coupling mode $V^2/t^2 \ll 1$. This simplification is quite appropriate, since graphene in the strong coupling mode ($V^2/t^2 \gg 1$) essentially disintegrates into independent carbon adatoms, thereby losing its unique properties.

Further estimates are obtained within the HOMO-LUMO [4] model, which is a simplified version of DBM: from the entire set of MM dangling orbitals, only the highest occupied (HOMO, ε_-) and the lowest unoccupied (LUMO, ε_+) orbitals are selected. The interaction of these orbitals with gapless epigraphene may then be characterized using Hamiltonian (1), where $i = +, -$, and (2) may be substituted with $\varepsilon'^{gap}_{gap}(\mathbf{k}) = \varepsilon'_D \pm \sqrt{\Delta^2 + (3tka/2)^2}$. Expression (3) takes the form

$$\rho_m^{gap}(\omega) = \frac{1}{\pi} \frac{\Gamma_m^{gap}(\omega')}{(\omega' - \varepsilon_m - \Lambda_m^{gap}(\omega'))^2 + (\Gamma_m^{gap}(\omega'))^2}, \qquad (12)$$

where $\omega' = \omega - \varepsilon'_D$. At zero temperature, the band contribution to occupation numbers $n_\mp^{gap}$ of HOMO and LUMO orbitals is

$$(h_\mp^{gap})_{band} = 2 \int\limits_{-\sqrt{\xi^2+\Delta^2}-\varepsilon'_D}^{-\Delta-\varepsilon'_D} \rho_\mp^{gap}(\omega) d\omega, \qquad (13)$$

while local contribution $(n_\mp^{gap})_{loc}$ is given by formula (8) with index i replaced by $\mp$, so that $\varepsilon_\mp^{loc} = \varepsilon_\mp + \Lambda_\mp^{gap}(\varepsilon_\mp^{loc})$. It should also be kept in mind that the position of the chemical potential in (8) is determined by the MM and gapped SLG, whereas the SiC substrate becomes an additional factor in the present case.

As an illustration, let us consider the case when the center of the band gap of the SiC polytype coincides with the Dirac point of gapped graphene and both materials are undoped; i.e., $\omega_0 = \varepsilon_D = \mu = 0$ [16]. There is no charge transfer between SiC and graphene in this scenario. Since $\Delta \ll E_g/2$ (straddling heterojunction), one may neglect the SiC substrate in the problem of local states and use the formulae from Section 1. Relying on Table. 2, we set $\varepsilon_- = -(I(\text{NO}) - \varphi_{SLG})$ and $\varepsilon_+ = -(A(\text{CH}_3) - \varphi_{SLG})$, where work function of graphene $\varphi_{SLG} = 4.5\,\text{eV}$ [1]. Then, $\varepsilon_- \approx -4.8\,\text{eV}$ and $\varepsilon_+ \approx -3.4\,\text{eV}$, which correspond to

Table 1. Band gap width E_g, position of its center ω_0 (relative to the Dirac point of free-standing graphene $\varepsilon_D = 0$), and energy of the shifted Dirac point $\varepsilon'_D = -\Lambda_{sub}(0)$ in eV

Polytype of SiC	8*H*	21*R*	6*H*	15*R*	27*R*	4*H*
E_g	2.86	2.96	3.00	3.06	3.13	3.23
$-\omega_0$	0.51	0.50	0.45	0.37	0.34	0.29
ε'_D	0.75	0.70	0.62	0.49	0.44	0.36

Table 2. Ionization I and electron affinity A energies of MM fragments in eV [17]

MM fragment	O_2	NO	NH	CH_2	NH_2	CH_3
I	12.07	9.26	13.1	10.4	10.15	9.84
A	0.44	0.03	0.37	0.65	0.76	1.07

$\varepsilon_{\pm}^{loc} \sim \mp\Delta$ and $\nu_{\pm}^{loc} \sim 0$. However, if we take image potential $V_{im} = e^2/4d$, where d is the distance between the MM fragment and graphene, into account (at $d = 2.5$ Å $V_{im} \sim 2$ eV), the ionization energy decreases ($I \to I - V_{im}$), while the affinity energy increases ($A \to A - V_{im}$) [18]. In this case, calculations are needed instead of order-of-magnitude estimates.

If we assume that it is the 3*D* substrate that dictates the μ value to the entire structure, an *n*- or *p*-type SiC substrate should be used to fill local levels ε_{-}^{loc} and ε_{+}^{loc}, respectively. If $T \neq 0$ and the chemical potential is close to a certain level ε_i^{loc}, an electron (hole) localized at this level may move to the conduction (valence) band when the temperature increases [19]. Thus, local levels in gapped graphene play the same role as impurity levels in a semiconductor.

Changes in the electronic states in a SiC-substrate -gapless SLG -antibody system caused by antigen–antibody bindings were discussed in [5]. It was hypothesized that the effect of an antigen on an antibody comes down to a shift in the energies of dangling bonds and a change in their broadening (or, in the present case, to a variation of the characteristics of HOMO and LUMO orbitals in formula (11)). It is impossible at present to calculate such changes, since the cross-linking of fragments of antibody and antigen biomolecules is performed by connector monomers (see Fig. 2 in [20]).

Concluding remarks

The SiC-SLG-biomolecule (acting as an antibody) system considered in the present study is a model of a biosensor in its initial state when the tested biomolecule (antigen) has not yet been brought into contact with the antibody. The antibody detection signal is the antigen-induced change in graphene conductivity $\sigma_{SLG} = en_{SLG}\mu_{SLG}$, where e is the elementary charge and n_{SLG} and μ_{SLG} are the concentration and the mobility of charge carriers. Gapless graphene features metallic conductivity, while gapped graphene is characterized by activation (semiconductor) conductivity. The activation nature of conductivity is associated with thermal delocalization of electrons from the ε_i^{loc} levels located inside the gap. Two ways of opening a gap in the graphene spectrum were mentioned above: deformation and the substrate effect. However, adsorption also allows one to functionalize graphene. Theoretically speaking, if the binding of an antigen to an antibody were to induce the emergence of a gap, this would be the best sensor operation mode, since a change in the graphene conductivity type is easier to detect than a conductivity variation (see formula (10) in [5], which, when applied to gapped graphene, should include the contribution of local states).

Funding

S.Yu. Davydov wishes to thank the Russian Science Foundation for financial support (grant 22-12-00134).

Conflict of interest

The authors declare that they have no conflict of interest.

References

[1] S.Yu. Davydov. Phys. Solid State, **64** (12), 2018 (2022). DOI: 10.21883/PSS.2022.12.54400.452
[2] I.V. Fntonova. Phys. Usp., **65**, 567 (2022).
[3] I.V. Antonova. Semiconductors, **50** (1), 66 (2016). DOI: 10.1134/S106378261601005X
[4] S.Yu. Dsvydov, A.A. Lebedev. Phys. Solid State, **65** (12), (2023).
[5] S.Yu. Davydov. Phys. Solid State, **66** (2), 293 (2024). DOI: 10.61011/PSS.2024.02.57928.251
[6] S.Yu. Davydov. Semicondyctors, **51** (2), 217 (2017). DOI: 10.1134/S1063782617020051
[7] S.Yu. Davydov. Phys. Solid State, **58** (6), 1222 (2016).

[8] S.Yu. Davydov, S.V. Troshin. Phys. Solid State, **49**, 1583 (2016). DOI: 10.1134/S1063783416040041
[9] F. Bechstedt, R. Enderlein. *Semiconductor surfaces and interfaces*. (Akademie-Verlag, Berlin, 1988), 441 p.
[10] S. Kim, J. Ihm, H.J. Choi, Y.-W. Son. Phys. Rev. Lett., **100**, 176802 (2008). DOI: 10.1103/PhysRevLett.100.176802
[11] X. Cao, J. Shi, M. Zhang, X. Jiang, H. Zhong, P. Huang, Y. Ding, M. Wu. J. Phys. Chem. C, **120**, 11299 (2016). DOI: https: 10.1021/acs.jpcc.6b03308
[12] R. Nandee, M.A. Chowdhury, A. Shahid, N. Hossain, M. Rana. Results in Engineer., **15**, 100474 (2022). www.sciencedirect.com/journal/results-in-engineering
[13] E.H. Hasdeo, L.P.A. Krisna, M.Y. Hanna, B.E. Gunara, N.T. Hung, A.R.T. Nugraha. J. Appl. Phys., **126**, 035109 (2019). DOI: 10.1063/1.5100985
[14] S.Yu. Davydov. Phys. Solid State, **58** (11), 1942 (2023). DOI: 10.61011/PSS.2023.11.57332.183
[15] S.Yu. Davydov. Phys. Solid State, **53** (4), 804 (2016). DOI: 10.1134/S1063783416040041
[16] S.Yu. Davydov, O.V. Posrednik. Semiconductors, **57** (9), 733 (2023).
[17] *Fizicheskie velichiny*, Ed. by E.S. Grigor'ev, E.Z. Meilikhov. (Energoatomizdat, M., 1991) (in Russian).
[18] *Theory of Chemisorption* ed. by J.R. Smith (Springer-Verlag, Berlin, 1980), Ch. 7.
[19] S.Yu. Davydov. Tech. Phys., **61** (7), 1106 (2016). DOI: 10.1134/S1063784216070100
[20] S.Yu. Davydov. Phys. Solid State, **66** (8), 1390 (2024). DOI: 10.61011/FTT.2024.08.58615.91

Translated by D.Safin